tion of the equilibrium stress-optical coefficients in connection with the light-scattering results shows that the reorganized regions should exhibit a higher form anisotropy the larger the value of M_{app}. Such increasing form anisotropy can be either due to increasing anisometry of the regions or—at a given anisometry—due to an increasing refractive index difference with the surrounding.

The reasons for the appearance of some fairly long-range anisotropic structures in the PHEMA hydrogels have previously, in the first place, been traced to the amphiphilic nature of the polymer chain, which especially in water could lead to regions of micromesomorphic order.[4] Inhomogeneous cross-linking may be a second contributing factor, especially if water is present during network formation.

The optical behavior can be qualitatively understood in terms of a somewhat organized network containing cross-links and entanglements. Any cross-link or entanglement will restrict the long-range organization. The movement of entanglements during stress relaxation will change the interchain correlations, so that a restructuring will result. At small M_{app} the equilibrium optical behavior will approach the Gaussian behavior because the large number of cross-links disrupts the organizing tendency of the amphiphilic system.

Acknowledgments. The financial support of the Syracuse University Research Institute is gratefully acknowleged. M. I. expresses his gratitude to the Institute of Macromolecular Chemistry, Czechoslovak Academy of Sciences, for granting a leave of absence, which made his postdoctoral stay in the U. S. possible. J. Hasa, Prague, has kindly cooperated in the preparation of the samples.

Light Scattering from a Two-Phase Polymer System. Scattering from a Spherical Domain Structure and Its Explanation in Terms of Heterogeneity Parameters[1a]

Masahiko Moritani,[1b] Takashi Inoue, Masahiko Motegi,[1c] and Hiromichi Kawai[1d]

Department of Polymer Chemistry, Faculty of Engineering, Kyoto University, Kyoto, Japan. *Received February 16, 1970*

ABSTRACT: The correlation function $\gamma(r)$ defined by Debye and Bueche for characterizing the inhomogeneity of solid materials is further investigated by measuring the intensity distribution of scattered light under the V_v polarization condition from the film specimens of block copolymers of styrene and isoprene (A–B type) and graft copolymers of butadiene and styrene–acrylonitrile (ABS resin type). Three kinds of heterogeneity parameters, "specific surface" S_{sp}, "distance of heterogeneity" $\bar{l}_e$, and "volume of heterogeneity" $\bar{\nu}$, as well as some statistical parameters, such as "short- and long-range correlation distances" a_1 and a_2 and "fractional contribution factors of short- and long-range fluctuations" f and $(1 - f)$, are determined from the intensity distribution of scattered light from the specimens, and are discussed in relation to the heterogeneity of the spherical domain structures of the specimens observed from their electron micrographs.

The heterogeneity in the structure of polymer solids greatly influences the bulk properties, and the light scattering may be a useful technique for quantifying the heterogeneity of the same dimensional order as the wavelength of the light used.

The theoretical studies of the light scattering from solid materials were first carried out by Debye and Bueche[2a] for an isotropic but inhomogeneous system, made more general by Goldstein and Michalik,[2b] and further extended by Stein and his coworkers[3–6] to the anisotropic system of crystalline polymers. In accordance with these theories, the intensity distribution of scattered light could give some statistical parameters which are related to the fluctuations of optical density and orientation within the system, *i.e.*, the heterogeneity and local anisotropy. However, the physical meaning of the parameters in relation to the heterogeneity of the system has not been fully understood, except for, for example, some indirect investigations where the parameters are compared with the results obtained from adsorption experiments.[7] This may be due to the lack of test specimens appropriate for making direct comparison of the parameters with the heterogeneity of the system.

Recent developments of synthesizing block and graft copolymers have made it possible to control the microphase separations of the block segments and of the grafted and backbone segments during casting the

(1) (a) Part of M.S. Thesis of M. Moritani presented to the Department of Polymer Chemistry, Faculty of Engineering, Kyoto University, March 10, 1970; presented partly before the 18th Annual Meeting of the Society of Polymer Science, Japan, Kyoto, May 20, 1969. (b) Niihama Mill, Shumitomo Chemical Co., Ltd., Niihama, Ehime-ken, Japan. (c) Film Laboratory, Toyo Rayon Co., Ltd., Ohtsu, Shiga-ken, Japan. (d) To whom all correspondence should be addressed.

(2) (a) P. Debye and A. M. Bueche, *J. Appl. Phys.*, **20**, 518 (1949); (b) M. Goldstein and E. R. Michlik, *ibid.*, **26**, 1450 (1955).

(3) R. S. Stein and M. B. Rhodes, *ibid.*, **31**, 1873 (1960).

(4) R. S. Stein and P. R. Wilson, *ibid.*, **33**, 1914 (1962).

(5) R. S. Stein, P. R. Wilson, and S. N. Stidham, *ibid.*, **34**, 46 (1963).

(6) R. S. Stein, P. Erhardt, J. J. van Aartsen, S. Clough, and M. B. Rhodes, *J. Polym. Sci., Part C*, **13**, 1 (1966).

(7) P. Debye, H. R. Anderson, and H. Brumberger, *J. Appl. Phys.*, **28**, 679 (1957).

copolymers into solid specimens.[8-15] In other words, it is possible to control the domain structures of the copolymers, microheterogeneous structures, not only in the shape but also in the size of the domains.

In this paper, the theory of light scattering from the density-fluctuating materials will be first checked in terms of the correlation function $\gamma(r)$, which was defined by Debye and Bueche, by measuring the intensity distribution of scattered light from the film specimens of block copolymers of styrene and isoprene (A–B type) and graft copolymers of butadiene and styrene–acrylonitrile (ABS resin type) both having well-controlled domain structures in colloidal dimensions. Then, heterogeneity and statistical parameters, which are further defined by approximating the correlation function $\gamma(r)$ to be given in a form of summation of short- and long-range fluctuations, will be discussed in relation to the heterogeneity of the domain structures of the specimens which is observed from their electron micrographs.

Test Specimens and Experimental Procedures

Figure 1 shows electron micrographs of ultrathin sections of the first series of test specimens having a domain structure of dispersed spheres of styrene component (white spheres unstained by OsO_4) within an isoprene matrix (black matrix stained by OsO_4). For this series, the diameters of the dispersed spheres are kept constant but the distance between the spheres is changed systematically to become wider in the order from specimens designated 20–80 block copolymer through hi 30. These are prepared by casting from 5% toluene solutions of binary systems of different compositions of the 20–80 block copolymer (A–B-type block copolymer of styrene and isoprene, $\bar{M}_n = 27.8 \times 10^4$, 18.5 wt % styrene) and a homopolyisoprene ($\bar{M}_n = 39.8 \times 10^4$), as indicated in a triangular diagram in the figure from 0 to 30 wt % homopolyisoprene.[11]

Figure 2 shows electron micrographs of ultrathin sections of the second series of test specimens having a domain structure of dispersed spheres of isoprene component within a styrene matrix. For this series, the volume fraction of the spherical domain is kept constant but the average diameter of the spherical domains is changed systematically to become larger in the order from Co 75 through Co 10. These are prepared by casting from 5% toluene solutions of ternary systems of different compositions of 70–30 block copolymer (A–B-type block copolymer of styrene and isoprene, $\bar{M}_n = 104 \times 10^4$, 73 wt % styrene), homopolystyrene ($\bar{M}_n = 143 \times 10^4$), and homopolyisoprene ($\bar{M}_n = 39.8 \times 10^4$), along an isopleth line in a triangular diagram in the figure; *i.e.*, the composition changes in fraction of the block copolymer from 75 to 10 wt % but the ratio of total styrene sequences to total isoprene sequences is identical with that of the copolymer, 73–27.[11]

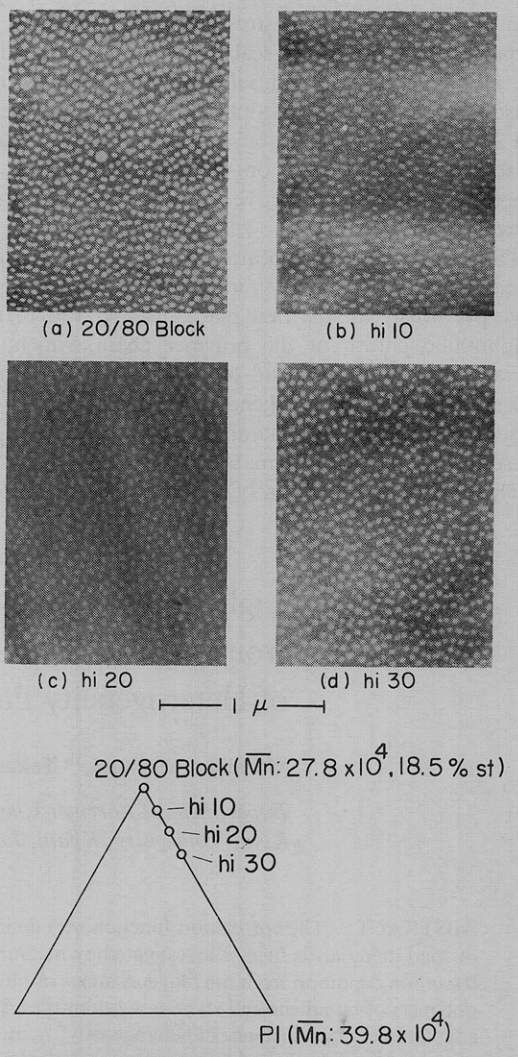

Figure 1. Electron micrographs of ultrathin sections of about 350 Å thickness cut normal to the surfaces of a series of test specimens prestained by OsO_4. The test specimens were cast from 5% toluene solutions of binary systems of different compositions of a 20–80 A–B-type block copolymer of styrene and isoprene and homopolyisoprene from 0 to 30 wt % homopolymer.

Figure 3 shows electron micrographs of ultrathin sections of a series of ABS lattices embedded in a mixture of polybutadiene and agar–agar and stained by OsO_4. The series of ABS lattices was made by a particular grafting technique in emulsion system of polybutadiene lattices dispersed in a medium containing styrene and acrylonitrile monomers so that the grafting occurs mostly onto the surface of the lattices, not within the lattices, and that the degree of grafting varies from 20 to 80 wt % for the series. As seen in the figure, polybutadiene spheres (black spheres stained by OsO_4) are surrounded by thicker layer of the grafted chains of styrene–acrylonitrile copolymer (white layer unstained by OsO_4) as the degree of grafting increase.[16]

(8) H. Hendus, K. H. Illers, and E. Ropte, *Kolloid-Z. Z. Polym.*, **216–217**, 110 (1967).
(9) M. Matsuo, S. Sagae, and H. Asahi, *Polymer*, **10**, 79 (1969).
(10) T. Inoue, T. Soen, T. Hashimoto, and H. Kawai, *J. Polym. Sci., Part A-2*, **7**, 1283 (1969).
(11) T. Inoue, T. Soen, T. Hashimoto, and H. Kawai, *Macromolecules*, **3**, 87 (1970).
(12) K. Kato, *J. Electronmicrosc.*, **14**, 219 (1965).
(13) G. Molau and H. Keskkula, *J. Polym. Sci., Part A-1*, **4**, 1595 (1966).
(14) R. J. Williams and R. W. A. Hudson, *Polymer*, **8**, 643 (1967).
(15) T. Ono, M. S. thesis presented to the Department of Polymer Chemistry, Faculty of Engineering, Kyoto University, March 11, 1969.
(16) K. Kato, *Jap. Plast.*, **19** (10), 89 (1968).

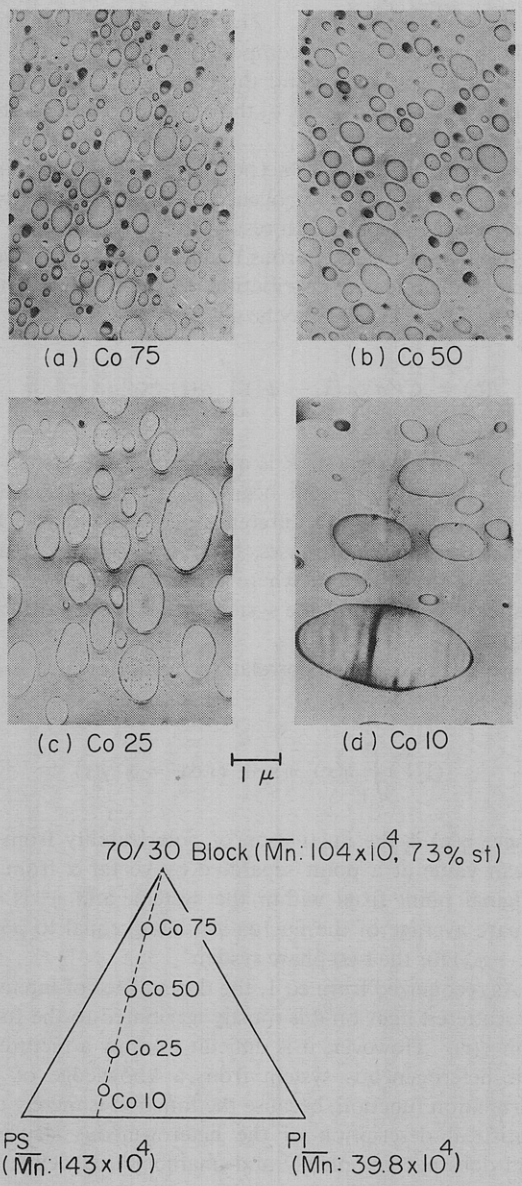

Figure 2. Electron micrographs of ultrathin sections of about 350 Å thickness cut normal to the surfaces of a series of test specimens prestained by OsO_4. The test specimens were cast from 5% toluene solutions of ternary system of a 70–30 A–B-type block copolymer of styrene and isoprene, homopolystyrene, and homopolyisoprene, differing in fraction of the block copolymer from 75 to 10 wt % but keeping the ratio of total styrene sequences to total isoprene sequences to be identical with that of the copolymer.

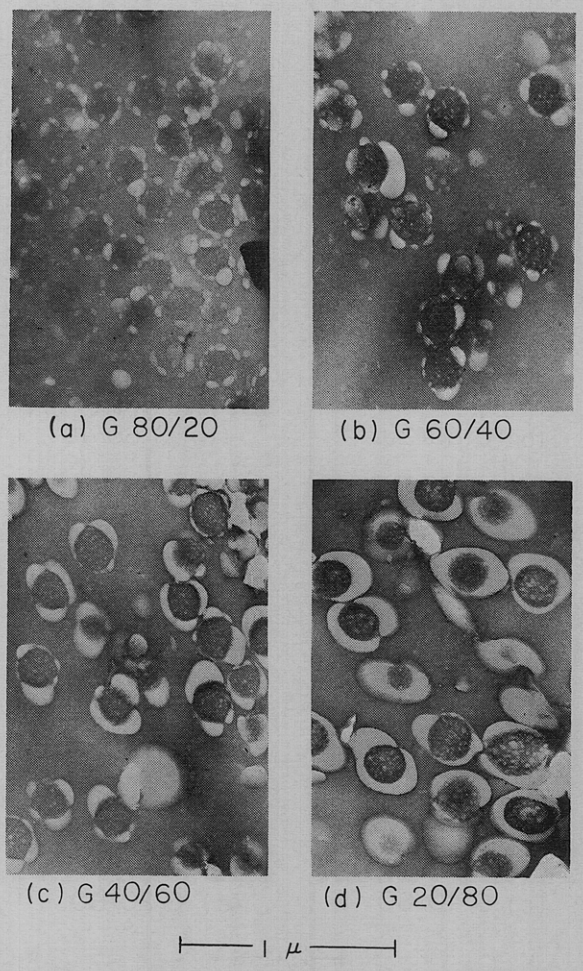

Figure 3. Electron micrographs of ultrathin sections of a series of ABS lattices embedded in a mixture of polybutadiene and agar–agar and stained by OsO_4. The series of ABS lattices was made so that the degree of grafting of styrene–acrylonitrile copolymer onto the surface of polybutadiene lattices varies from 20 to 80 wt %.

Figure 4 shows electron micrographs of ultrathin sections of the third series of test specimens cast from 5% monochlorobenzene solutions of mixtures of a styrene–acrylonitrile copolymer, whose molecular composition is the same as that of the grafted copolymer, with each ABS latex. For mixing the two components, the fraction of each ABS latex was controlled so that the weight fraction of polybutadiene is always kept constant, as a whole, as 20% for every specimen. As seen in the figure, the spherical domains of polybutadiene (black spheres stained by OsO_4) which are dispersed in a matrix of styrene–acrylonitrile copolymer (white matrix unstained by OsO_4) are very uniform in size for every specimen, but less uniformly dispersed as the degree of grafting of the ABS latex decreases. This systematic change of dispersity should be understood, as suggested in the previous paper,[11] in terms of the coalescence barrier which prevents demixing of the polymeric oil-in-oil emulsion of ABS lattices in the monochlorobenzene solution of the styrene–acrylonitrile copolymer during the casting of the system. That is, the greater the degree of grafting on the ABS lattices, the stronger the entropic repulsion between approaching droplets of the ABS lattices becomes resulting in the more uniform dispersion of the spherical domains of polybutadiene in the matrix of styrene–acrylonitrile copolymer. This repulsion arises, as suggested by Clayfield[17a] and Meier,[17b] from a decrease in the configurational entropy of the grafted chain due to the loss of possible configurations as the space available to the grafted chains is reduced between the approaching droplets.

The test specimens, which were cast into films of about 0.1 mm thickness, were placed normal to the incident beam, provided by a He–Ne gas laser apparatus, Model

(17) (a) E. J. Clayfield and E. C. Lumb, *J. Colloid Interface Sci.*, 22, 269 (1966); (b) D. J. Meier, *J. Phys. Chem.*, 71, 1861 (1967).

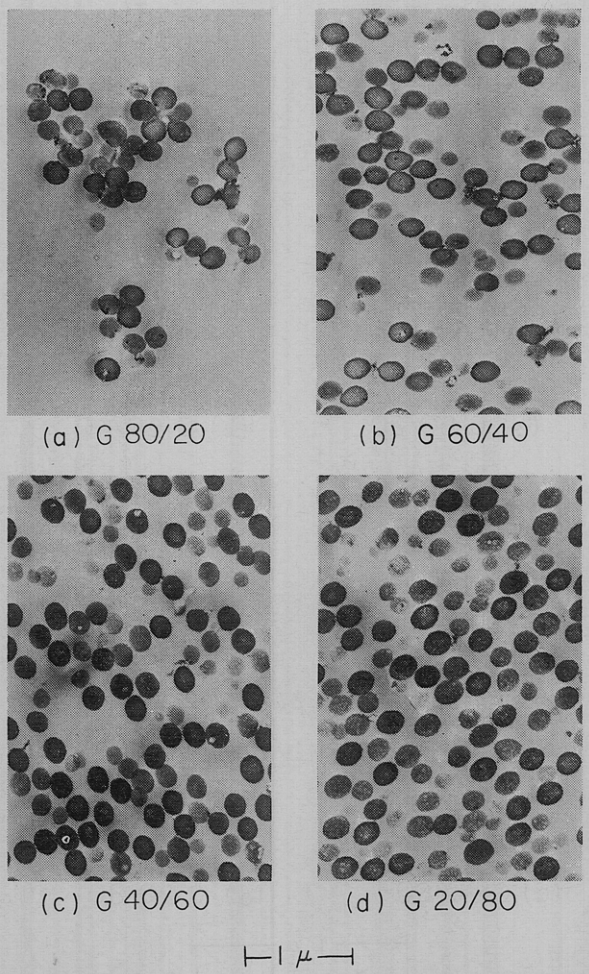

Figure 4. Electron micrographs of ultrathin sections of about 350 Å thickness cut normal to the snrfaces of a series of test specimens prestained by OsO_4. The test specimens were cast from 5% monochlorobenzene solutions of mixtures of a styrene–acrylonitrile copolymer with each ABS latex in Figure 3. For mixing the two components, the fraction of each latex was controlled so that the weight fraction of polybutadiene was always kept constant, as a whole, as 20% for every specimen.

NAL-705Z, Nippon Kakaku Kogyo Inc. The incident beam was well collimated, polarized to the vertical direction by using a polarization rotator, Model 310, Spectra Physics Inc., and monochromatized at a wavelength of 6328 Å. The intensity of scattered light from the specimen was detected as function of scattering angle θ and azimuthal angle Ω by scanning with a phototube in a horizontal plane and rotating the specimen around its film normal, respectively. The analyzer was placed just before the phototube so that its polarization direction can be rotatable within a plane perpendicular to the scattered ray at a given θ and that any combination of polarization condition, such as V_v and H_v polarization, can be achieved. For the experiments, however, the V_v polarization condition was mainly used because of very weak H_v scattering being probably due to the smallness of the local anisotropy of the system.

Theory

As seen in the electron micrographs in Figures 1, 2, and 4, every specimen has a definite two-phase structure of dispersed spheres of one component within a matrix of the other component. The difference of refractive indices between the two components is very small for all of the test specimens, and the treatment proposed by Guinier, *et al.*,[18] in terms of the Rayleigh–Gans scattering may be applicable.

Applying the Debye–Bueche theory of light scattering from isotropic but inhomogeneous system[2a] to the two-phase system, an identical result with that calculated by Debye, *et al.*, for the porous materials[7] can be derived. That is, the intensity distribution of scattered light from the two-phase system may be given by

$$I(\mathbf{h}) = CV\rho^2\phi_A(1 - \phi_A)\int_V \gamma(\mathbf{r}) \exp[i(\mathbf{h}\cdot\mathbf{r})]\, d\mathbf{r} \quad (1)$$

where C is a constant, V is a volume of the system irradiated by the incident beam, ϕ_A is volume fraction of the A phase, ρ is a difference of polarizabilities between the A and B phases, $\mathbf{h} = k\mathbf{s}$, $k = 2\pi/\lambda'$, and $|\mathbf{s}| = 2 \sin(\theta/2)$ and where λ' is wavelength of the scattered light within the system and θ is the scattering angle.

$\gamma(\mathbf{r})$ is the so-called correlation function which is defined by

$$(1/V)\int_V \eta(\mathbf{x})\cdot\eta(\mathbf{x} + \mathbf{r})\, d\mathbf{x} = \overline{\eta^2}\gamma(\mathbf{r}) \quad (2)$$

where $\eta(\mathbf{x})$ is the fluctuation of polarizability from its mean value at a point separated by vector $\mathbf{x}$ from an original point fixed within the system, and $\overline{\eta^2}$ is the square average of the fluctuation being equal to $\rho^2\phi_A(1 - \phi_A)$ for the two-phase system.

As recognized from eq 1, the dependence of intensity of scattered light on θ is mostly attributed to the function $\gamma(\mathbf{r})$. However, it is difficult to draw a picture of this heterogeneous system from a knowledge of the correlation function, because the function is merely one statistical description of the heterogeneous structure and does not completely and unambigously define the structure. In order to introduce some statistical parameters having simple but discrete meaning rather than $\gamma(\mathbf{r})$, it is necessary to discuss the statistical property of the function in more detail for a particular case of the domain structure of dispersed spheres of one component within a matrix of the other component.

Now, let us consider a two-phase system of volume V, in which N spheres of A component are dispersed in uniform size (radius R_0 and volume v) within a matrix of B component, and define a probability function $Z_{AA}(\mathbf{r})$ to find an A point separated from the other point by a vector $\mathbf{r}$. The function has nondirectional dependence for the isotropic system, *i.e.*, just a function of distance r, so that the function may be unity when $r = 0$ and be ϕ_A as $r \to \infty$, unless there is a long-range correlation. The function may be written by

$$Z_{AA}(r) = \phi_A + (1 - \phi_A)\gamma(r) \quad (3)$$

It may be easily shown that $\gamma(r)$ in eq 3 is identical with the function defined by eq 2.[7]

A probability function $Z_{AA_i}(\mathbf{r})$ to find an A point

(18) A. Guinier and G. Fournet, "Small-Angle Scattering of X-Rays," Wiley, New York, N. Y., 1955, Chapter 2.

separated by vector **r** from the other A point fixed within the ith sphere may be given by

$$Z_{AA_i}(\mathbf{r}) = \gamma_0(\mathbf{r}) + \sum_{j \neq i} \gamma_0(\mathbf{r} - \mathbf{R}_{ij}) \tag{4}$$

where $\gamma_0(\mathbf{r})$ and $\gamma_0(\mathbf{r} - \mathbf{R}_{ij})$ are volume fractions of the ith sphere superposed by its original sphere and the ith sphere, respectively, when the ith sphere is moved by the vector **r** from its original position, as illustrated in Figure 5, and where $\mathbf{R}_{ij}$ is a position vector of the jth sphere with respect to the ith sphere. For the A sphere, $\gamma_0(\mathbf{r})$ may be a function only of r and is given by

$$\gamma_0(r) = 1 - (3/4)(r/R_0) + (1/16)(r/R_0)^3 \tag{5}$$

When the spheres are dispersed randomly, $Z_{AA_i}(\mathbf{r})$ must be identical for every sphere and be equal to $Z_{AA}(\mathbf{r})$. But when the spheres are dispersed in not random, $Z_{AA_i}(\mathbf{r})$ must be averaged over all of the spheres to give

$$Z_{AA}(\mathbf{r}) = (1/N)\sum_i \left[\gamma_0(\mathbf{r}) + \sum_{j \neq i} \gamma_0(\mathbf{r} - \mathbf{R}_{ij})\right] \tag{6}$$

A representation of eq 6 in the form of integration may be given by

$$Z_{AA}(\mathbf{r}) = \gamma_0(\mathbf{r}) + \frac{N-1}{V}\int_V G(\mathbf{R})\gamma_0(\mathbf{r} - \mathbf{R})\, d\mathbf{R} \tag{7}$$

where $G(\mathbf{R})$ is a function defined by

$$G(\mathbf{R})\, d\mathbf{R} \equiv \frac{V}{N(N-1)}\left[\int P_i(\mathbf{R})\, dv_i\right] d\mathbf{R} \tag{8}$$

and where $P_i(\mathbf{R})$ is a probability function to find a pair of centers of spheres; one is in a volume element dv_i and the other is in a volume element $d\mathbf{R}_i$ separated by the vector **R** from the dv_i.

Substituting eq 6 into eq 3, $\gamma(\mathbf{r})$ can be represented by

$$\gamma(\mathbf{r}) = \frac{1}{1-\phi_A}\left\{\gamma_0(\mathbf{r}) + \frac{N-1}{V}\int_V [G(\mathbf{R}) - 1] \times \gamma_0(\mathbf{r} - \mathbf{R})\, d\mathbf{R} - (v/V)\right\} \tag{9}[19]$$

Defining a density function $Q(\mathbf{x})$ representing the number of spheres included in a volume element $d\mathbf{x}$ separated by vector **x** from the original point fixed within the system, the fluctuation of $Q(\mathbf{x})$ from its average, $Q_0\,(= N/V)$, can be given by

$$\xi(\mathbf{x}) = \frac{Q(\mathbf{x}) - Q_0}{Q_0} \tag{10}$$

which further gives the relation

$$\int_V P_i(\mathbf{R})\, dv_i = \int_V Q(\mathbf{x}) \cdot Q(\mathbf{x} + \mathbf{R})\Phi(\mathbf{R})\, d\mathbf{x} = \Phi(\mathbf{R})Q_0{}^2V\left[1 + (1/V)\int_V \xi(\mathbf{x}) \cdot \xi(\mathbf{x} + \mathbf{R})\, d\mathbf{x}\right] \tag{11}$$

(19) Substituting eq 9 into eq 1 and using a theorem that the Fourier transform of a faltung is the product of the transforms, $I(\mathbf{h})$ is given by

$$I(\mathbf{h}) \cong [\int \gamma_0(\mathbf{r}) \exp(i\mathbf{hr})\, d\mathbf{r}] \times [1 + (N/V)\int [G(\mathbf{R}) - 1] \exp(i\mathbf{hR})\, d\mathbf{R}]$$

That is to say, Zernicke–Prins type of equation[18] is obtained.

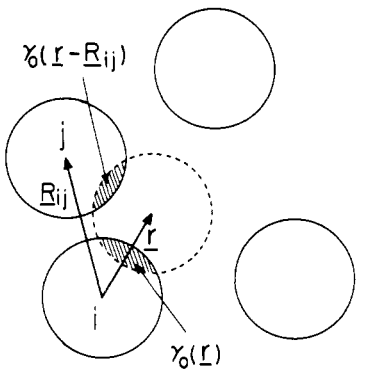

Figure 5. Schematic diagram showing the fractional volumes of the ith sphere superposed by its original sphere and the jth sphere, when the ith sphere is moved with the vector **r**.

where $\Phi(\mathbf{R})$ is a function representing an excluded volume effect by the sphere. For a rigid sphere, $\Phi(\mathbf{R})$ is a sort of cutoff function being zero for the inside of its own sphere and unity for the outside of the sphere, *i.e.*, $\Phi(\mathbf{R}) = 0$ for $0 \leqq |\mathbf{R}| \leqq 2R_0$ and $\Phi(\mathbf{R}) = 1$ for $2R_0 \leqq |\mathbf{R}|$.

Let us introduce two additional functional functions, $\Phi'(\mathbf{R})$ and $B(\mathbf{R})$, defined as

$$1 - \Phi(\mathbf{R}) = \Phi'(\mathbf{R}) \tag{12}$$

and

$$\frac{1}{V}\int_V \xi(\mathbf{x}) \cdot \xi(\mathbf{x} + \mathbf{R})\, d\mathbf{x} = \langle\xi^2\rangle B(\mathbf{R}) \tag{13}$$

where $\langle\xi^2\rangle$ is a square average given by $(1/V)\int_V [\xi(\mathbf{x})]^2 d\mathbf{x}$.

The function $B(\mathbf{R})$, which corresponds to the fluctuation of number density of spheres within the system, seems to change with slow decreasing for longer distance than $2R_0$ but be almost constant for a range of $0 \leqq |\mathbf{R}| \leqq 2R_0$, where $\Phi'(\mathbf{R})$ is not zero. This deduces the following relation through eq 8, 11 and 13

$$G(\mathbf{R}) - 1 \cong \frac{N}{N-1}[-\Phi'(\mathbf{R})(1 + \langle\xi^2\rangle) + \langle\xi^2\rangle B(\mathbf{R})] + 1/(N-1) \tag{14}$$

Substituting eq 14 into eq 9, the correlation function $\gamma(\mathbf{r})$ can be finally represented by

$$\gamma(\mathbf{r}) = \frac{1}{1-\phi_A}\left\{\gamma_0(\mathbf{r}) - \frac{\phi_A(1 + \langle\xi^2\rangle)}{v}\int_V \Phi'(\mathbf{R})\gamma_0 \times (\mathbf{r} - \mathbf{R})\, d\mathbf{R}\right\} + \frac{\langle\xi^2\rangle\phi_A}{(1-\phi_A)v}\int_V B(\mathbf{R})\gamma_0(\mathbf{r} - \mathbf{R})\, d\mathbf{r} \tag{15}$$

Assuming that A sphere is rigid enough, the first term in the right-hand side of eq 15 can be deduced for $0 \leqq |\mathbf{R}| \leqq 2R_0$ to give the relation

$$\text{(the first term)} = f - \frac{Sr}{4(1-\phi_A)} - \left[\frac{3}{16}f - \frac{1}{4(1-\phi_A)}\right](r/R_0)^3 + \frac{9}{160}\left(f - \frac{1}{1-\phi_A}\right)(r/R_0)^4 - \frac{1}{2240}\left(f - \frac{1}{1-\phi_A}\right)(r/R_0)^6 \tag{16}$$

where S is specific surface of the dispersed spheres represented by

$$S = \frac{4\pi R_0^2}{(4/3)\pi R_0^3} = 3/R_0 \tag{17}$$

and f is a quantity given by

$$f = 1 - \frac{\phi_A}{1 - \phi_A}\langle \xi^2 \rangle \tag{18}$$

which becomes unity when the fluctuation $\langle \xi^2 \rangle$ is so small as to approach zero, and, in contrast, becomes less than unity when the fluctuation is large.

The first term in the right-hand side of eq 15, which is represented by eq 16 for a rather short range of $|\mathbf{R}|$, *i.e.*, $0 \leqq |\mathbf{R}| \leqq 2R_0$, may be approximated as an exponential function by omitting the higher terms than the second in eq 16 for small value of $|\mathbf{r}|$.[20] This gives

$$\text{(the first term)} = f \exp\left[\frac{-S_{sp}r}{4(1 - \phi_A)\phi_A f}\right] = f \exp(-r/a_1) \tag{19}$$

where S_{sp} is the "specific surface" representing the interfacial area between the two phases per unit volume of the system and is considered as one of the heterogeneity parameters of the system, and a_1 is a quantity given by

$$a_1 = \frac{4(1 - \phi_A)\phi_A f}{S_{sp}} \tag{20}$$

As recognized from the derivation of eq 19, a_1 is a correlation distance of short-range fluctuation of optical density arising from the spherical domain itself, mostly from its intersurface to the matrix.

$\gamma_0(\mathbf{r} - \mathbf{R})$ must be a peak function as compared with $B(\mathbf{R})$ so that it may be approximated by the Dirac δ function at $\mathbf{r} = \mathbf{R}$. Therefore, the second term in the right-hand side of eq 15 may be approximated as

$$\text{(the second term)} = (1 - f)B(\mathbf{r}) \tag{21}$$

The function $B(\mathbf{R})$ may be postulated as a Gaussian-type function given by the following representation for the isotropic system

$$B(\mathbf{r}) = \exp[-(r/a_2)^2] \tag{22}$$

where a_2 is a correlation distance of long-range fluctuation of optical density arising from the correlation of the dispersed spheres.

From the above results, the correlation function $\gamma(\mathbf{r})$ given by eq 15 can be approximated for the isotropic system by summing eq 19 and 22 to give

$$\gamma(r) = f \cdot \exp(-r/a_1) + (1 - f) \cdot \exp[-(r/a_2)^2] \tag{23}$$

As seen in eq 23, the quantity f defined by eq 18 plays the role of a fractional contribution factor of the short-range fluctuation to the correlation function.

Integrating $Z_{AA}(r)$ over a range of r from 0 to L, *i.e.*

$$\int_0^L Z_{AA}(r)\,dr = L\phi_A + (1 - \phi_A)\int_0^L \gamma(r)\,dr \cong L\phi_A + (1 - \phi_A)\int_0^\infty \gamma(r)\,dr \tag{24}$$

when L is large enough, and defining

$$\int_0^\infty \gamma(r)dr \equiv \bar{l}_c/2$$

then $\bar{l}_c$ is a parameter to characterize the "distance of heterogeneity" of the system.

Furthermore, integrating $Z_{AA}(r)4\pi r^2$ over a range of r from 0 to R, *i.e.*

$$\int_0^R Z_{AA}(r)4\pi r^2\,dr = V\phi_A + (1 - \phi_A)\int_0^R \gamma(r)4\pi r^2\,dr \cong V\phi_A + (1 - \phi_A)\int_0^\infty \gamma(r)4\pi r^2\,dr \tag{25}$$

when R is large enough, and defining

$$\int_0^\infty \gamma(r)4\pi r^2 dr \equiv \bar{v}$$

then $\bar{v}$ is a parameter to characterize the "volume of heterogeneity" of the system.

The heterogeneity parameters, S_{sp}, $\bar{l}_c$, and $\bar{v}$, defined as the above, represent the surface area of a sphere, its size and volume, respectively, when the sphere is isolated in a very dilute system.

$\gamma(r)$ may be determined from $I(\mathbf{h})$ by means of the Fourier transformation of eq 1, provided that $I(\mathbf{h})$ is obtained for a wide range of $|\mathbf{h}|$. This seems, however, to be difficult from an experimental point of view, especially for large values of $|\mathbf{h}|$. Let us determine experimentally the statistical parameters, a_1, a_2, and f, and the three heterogeneity parameters, S_{sp}, $\bar{l}_c$, and $\bar{v}$, from $I(\mathbf{h})$ on the basis of approximating $\gamma(r)$ as the summation given by eq 23.[21]

The intensity distribution of scattered light from the isotropic system can be deduced from eq 1 as follows

$$I(h) = CV\rho^2\phi_A(1 - \phi_A)\int_0^\infty \gamma(r)\frac{\sin(hr)}{hr}4\pi r^2\,dr \tag{26}$$

Substituting eq 23 into eq 26, the intensity distribution of scattered light may be given by

$$I(h) = CV\rho^2\phi_A(1 - \phi_A)4\pi\{(2fa_1^3)/[1 + (ksa_1)^2]^2 + (1 - f)(\pi^{1/2}a_2^3/4)\exp[-(ksa_2/2)^2]\} \tag{27}$$

As recognized from eq 27, the plot of $I^{-1/2}$ against s^2 gives a linear relationship at large scattering angles, providing that the contribution of the second term in

(20) In the above discussions on $\gamma(\mathbf{r})$, every statistical function was defined in terms of the vector quantities of $\mathbf{r}$ or/and $\mathbf{R}$, but for such isotropic system as discussed here to have nondirectional dependence of the heterogeneity, the vector quantities may be replaced by the scalar quantities, such as $|\mathbf{r}|$, $|\mathbf{R}|$, and $|\mathbf{r} - \mathbf{R}|$.

(21) From an experimental point of view, there have been several proposals for the expression of $\gamma(r)$ in terms of either of an exponential,[22,23] or a Gaussian-type function,[23,24] or summation of the two functions.[7]

(22) J. J. Keane and R. S. Stein, *J. Polym. Sci.*, **20**, 327 (1956).

(23) A. E. M. Keijzers, J. J. van Aartsen, and W. Prins, *J. Appl. Phys.*, **36**, 2874 (1965).

(24) E. V. Beebe, R. L. Coalson, and R. H. Marchessault, *J. Polym. Sci., Part C*, **13**, 103 (1966).

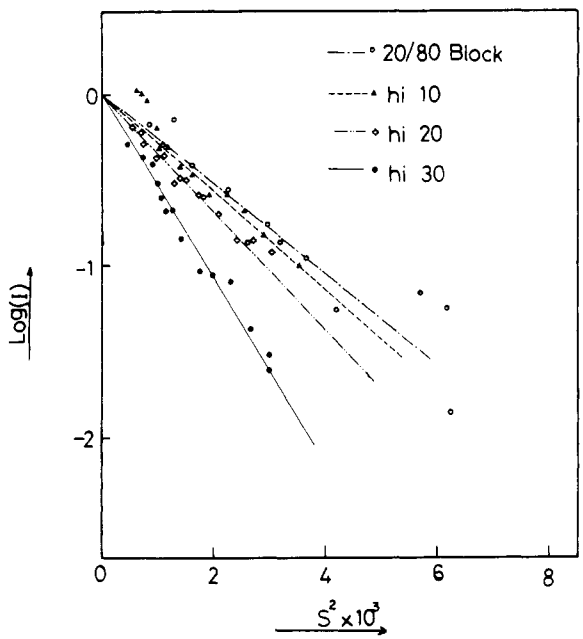

Figure 6. The intensity distribution of scattered light along the scattering angle in terms of the plot of log (I) *vs.* s^2 for a series of test specimens in Figure 1 differing in concentration but being identical in diameter of the dispersed spheres.

the right-hand side in eq 27 is much smaller than the first one, from which the parameter a_1 may be determined as

$$a_1 = (\lambda'/2)\left(\frac{\text{slope of the linear relationship}}{\text{intercept of the linear relationship at } s^2 = 0}\right)^{1/2} \quad (28)$$

The plot of the logarithm of the difference between the observed intensity $I(h)$ and the intensity calculated from the first term in the right-hand side in eq 27 against s^2 gives also a linear relationship, from which the parameter a_2 may be determined as

$$a_2 = (\lambda'/\pi)\left(\frac{\text{slope of the linear relationship}}{0.4343}\right)^{1/2} \quad (29)$$

The fractional contribution factor f may be given by

$$f = [1 + (8/\pi^{1/2})(a_1/a_2)^3 A]^{-1} \quad (30)$$

where A is the ratio of the Gaussian term to the exponential term at $\theta = 0°$, and is given by

$$A = [(1 - f)\pi^{1/2}a_2^3/4]/(2fa_1^3) \quad (31)$$

The relationship between the parameters a_1, a_2, and f, and the parameters S_{sp}, $\bar{l}_c$, and $\bar{v}$, may be given by

$$f/a_1 = S_{sp}/[4\phi_A(1 - \phi_A)] \quad (32)$$

$$\bar{l}_c/2 = fa_1 + (1 - f)a_2\pi^{1/2}/2 \quad (33)$$

$$\bar{v} = 4[2fa_1^3 + (1 - f)\pi^{1/2}a_2^3/4] \quad (34)$$

Results and Discussion

For every specimen, the intensity distribution of scattered light was measured under V_v polarization conditions. There was hardly any variation of the intensity with azimutal angle, confirming the isotropy of the system to have nondirectional dependence of the heterogeneity.

TABLE I
THE VALUE OF a_2 DETERMINED FROM EQUATION 29[a]

Parameter,	Specimen			
	20–80 block	hi 10	hi 20	hi 30
a_2, μ	1.01	1.06	1.17	1.43

[a] Using the slope of linear relationship between log (I) and s^2 for the first series of test specimens in Figure 1.

In order to discuss the parameter a_2, the long-range correlation distance, the intensity distribution of scattered light from the first series of test specimens in Figure 1 was measured under the V_v polarization condition. Figure 6 shows the intensity variation with the scattering angle in terms of the plot of log (I) *vs.* s^2.[25] The values of a_2 determined from eq 29 by using the slope of this linear plot are listed in Table I for the series of test specimens, 20–80 block, hi 10, hi 20, and hi 30. As seen in the table, a_2 becomes larger as the concentration of the dispersed spheres decreases, *i.e.*, as the distance between the spheres becomes large.

In order to discuss the other parameters, the intensity distribution of scattered light from the second series of test specimens in Figure 2 was measured also under the V_v polarization condition. Figure 7 shows the intensity variation with the scattering angle in terms of the plot of $(I)^{-1/2}$ against s^2. As seen in the figure, the linear relationship at large scattering angles, as expected for deducing eq 28 from eq 27, is followed. The separation of the scattering angle dependence of the intensity into two parts, at small and large scattering angles, becomes obvious as the size of the dispersed spheres

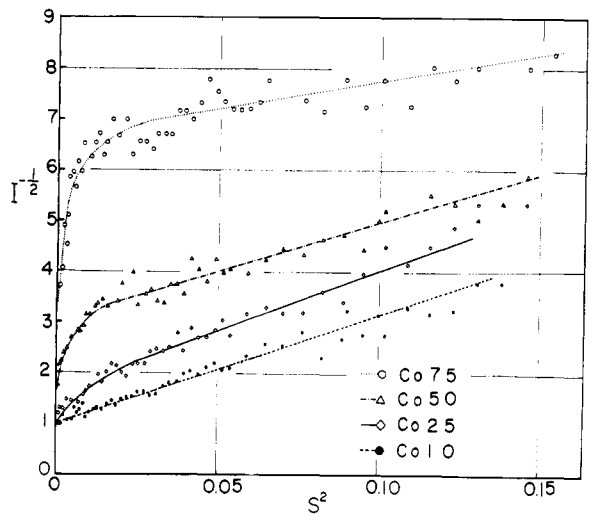

Figure. 7. The intensity distribution of scattered light along the scattering angle in terms of the plot of $(I)^{-1/2}$ *vs.* s^2 for a series of test specimens in Figure 2 differing in diameter but being identical in volume fraction of the dispersed spheres.

(25) Here, log (I), not log (I_{diff}) as used for deducing eq 31, is plotted against s^2. However, the contribution of the first term in the right-hand side of eq 27 at a small angle is usually very small so that the value of a_2 is hardly affected by this omission.

TABLE II
THE VALUES OF THE HETEROGENEITY AND STATISTICAL PARAMETERS[a]

Parameters	Specimen Co 75	Co 50	Co 25	Co 10
a_1, Å	885	1870	2490	3020
a_2, μ	1.2	1.6	1.5	
f	0.999	0.983	0.985	
S_{sp}, μ^{-1}	9.48	4.42	3.32	2.78
$\bar{l}_c$, Å	1980	4000	5400	6040
$\bar{v} \times 10^9$, Å^3	30	370	660	690
R_{scatt}, Å	936	2010	2670	3230
$R_{E.M.}$, Å	1270	1610	2710	3550

[a] Determined from eq 28–34 from the second series of test specimen in Figure 2.

becomes small. In other words, the rapid decrease at small scattering angles diminishes to make the dependence just a linear relationship as the size of the dispersed spheres becomes large.

The heterogeneity parameters determined from the results by using eq 28–34 are listed in Table II for the second series of test specimens, Co 75, Co 50, Co 25, and Co 10. As seen in the table, a_2 is much larger than a_1 for every specimen, ranging around 1 μ. The value of f is very close to unity for every specimen, which suggests that the fluctuation of optical density is mostly ascribed to the fluctuation in the short-range correlation. The heterogeneity parameters, $\bar{l}_c$ and $\bar{v}$, become large, and, in contrast, S_{sp} becomes small as the size of the dispersed spheres becomes large. R_{scatt} is a mean diameter of the dispersed spheres determined from S_{sp}. The comparison of the R_{scatt} with $R_{E.M.}$, which is determined directly from the electron micrograph in Figure 2, is shown in Figure 8, giving a fairly good linear relationship passing through the origin with a slope of 45°.

Furthermore, in order to discuss the parameters in more detail, the intensity distribution of scattered light from the third series of test specimens in Figure 4, for which the spherical domains are dispersed in different regularity but the size of the domain is kept uniform and the volume fraction of the domains is kept constant, was also measured. The values of the parameters determined from the same procedures as the above are listed in Table III.

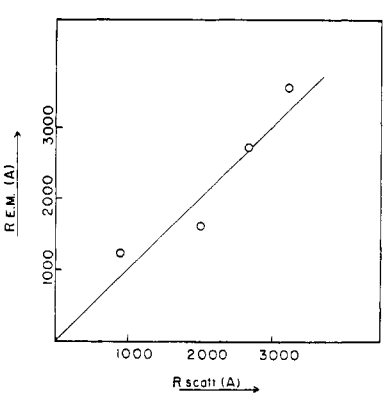

Figure 8. A plot of R_{scatt}, determined from S_{sp}, against $R_{E.M.}$, determined from an electron micrograph, for a series of test specimens in Figure 2, giving a fairly good linear relationship passing through the origin with a slope of 45°.

TABLE III
THE VALUES OF THE HETEROGENEITY AND STATISTICAL PARAMETERS[a]

Parameters	Specimen G 20–80	G 40–60	G 60–40	G 80–20
a_1, Å	1350	1500	1900	2000
a_2, μ	1.38	1.34	1.16	1.13
f	0.994	0.983	0.944	0.918
$\bar{l}_c$, Å	2830	3340	5140	5320
$\bar{v} \times 10^9$, Å^3	149	296	651	845

[a] Determined from eq 28–34 for the third series of test specimens in Figure 4.

As recognized from Table III, the less uniform the dispersion of the spherical domains, the greater the value of a_1, the short-range correlation distance, which increases in the order from *G* 20–80, *G* 40–60, *G* 60–40, and *G* 80–20. This must be understood, as expected from eq 20 or 32, in terms of the local coalescence of the dispersed spheres, which decreases the "specific surface" S_{sp} of the system when the dispersion becomes less uniform. In contrast, the more uniform the dispersity, the greater become the values of a_2 and f, the long-range correlation distance and the fractional contribution factor of the short-range fluctuation to the total fluctuation $\gamma(r)$. In other words, the more uniform the dispersity of the spherical domains, the smaller the contribution of the long-range fluctuation to the total fluctuation becomes, as expected from eq 18 in terms of the decrease of $\langle \xi^2 \rangle$, being accompanied with the increase of the long-range correlation distance. In addition, the "distance of heterogeneity" $\bar{l}_c$ and the "volume of heterogeneity" $\bar{v}$ increase as the dispersion becomes less uniform.

Any quantitative discussion on the "specific surface" S_{sp} of the third series of the specimens, as listed in Table II for the second series of test specimens, may be meaningless, because of some possibility of polymerization of styrene–acrylonitrile copolymer within the spherical domains of polybutadiene, as seen in the electron micrographs in Figure 4, which must affect the value of S_{sp} in an unexpected direction.

Conclusion

The theory of light scattering from a heterogeneous system having density fluctuation but nondirectional dependence of the heterogeneity (isotropic) was checked in terms of the correlation function $\gamma(r)$. The function was approximated to be given by summation of short- and long-range fluctuations, which were represented by an exponential function with a short-range correlation distance a_1 and a Gaussian-type function with a long-range correlation distance a_2, respectively. The validity of the approximation was first investigated by measuring the V_v intensity variation of scattered light from the films of definite two-phase polymer systems having a domain structures of dispersed spheres of one component within a matrix of the other component but differing in either concentration of the dispersed spheres, size of the spheres in a range of colloidal dimensions, or uniformity of the dispersion of the spheres in the matrix.

It was found that the contribution of the long-range fluctuation to the total fluctuation $\gamma(r)$ is usually very small, ranging around a few per cent, and that a_2, which reaches $\sim 1\ \mu$, is much larger than a_1 varying from several hundred to a few thousand ångströms with good correlation to the size of the dispersed spheres.

Three kinds of heterogeneity parameters, "specific surface" S_{sp}, "distance of heterogeneity" $\bar{l}_c$, and "volume of heterogeneity" $\bar{v}$, which were further defined from the correlation function $\gamma(r)$, as well as the statistical parameters, such as a_1 and a_2, and the fractional contribution factors of the short- and long-range fluctuations, f and $(1 - f)$, were discussed in relation to the heterogeneity of the colloidal domain structures of the specimens observed from their electron micrographs.

The following conclusions were obtained. The larger the size of the spherical domain, the larger the correlation distances, a_1 and a_2, as well as the heterogeneity parameters, $\bar{l}_c$ and $\bar{v}$, and, in contrast, the smaller the specific surface S_{sp}. The larger the distance between the dispersed spherical domains, the larger the long-range correlation distance. The less uniform the dispersion of the spherical domains, the larger the short-range correlation distance a_1 as well as the heterogeneity parameters, $\bar{l}_c$ and $\bar{v}$, and, in contrast, the smaller the long-range correlation distance a_2 and the fractional contribution factor of the long-range fluctuation $(1 - f)$. The radius of the dispersed spheres R_{scatt}, which is determined from the parameter S_{sp}, agrees fairly well with $R_{E.M.}$ determined from the electron micrograph of the domain structures.

Acknowledgments. The authors are deeply indebted to Dr. K. Kato and Mr. M. Nishimura, Central Research Laboratory, Toyo Rayon Co. Ltd., for kindly arranging for preparation of the electron micrographs.

A part of this work was supported by the grant from the Scientific Research Funds (Kagaku Kenkyu-hi, 19214-1967) of the Ministry of Education, Japan, and the grant from the Japan Synthetic Rubber Co. Ltd., Tokyo, Japan.

Structure of Isotactic Poly(methyl methacrylate)

Hiroyuki Tadokoro, Yôzô Chatani, Hiroshi Kusanagi, and Masaaki Yokoyama

Department of Polymer Science, Faculty of Science, Osaka University, Toyonaka, Osaka, Japan. *Received March 16, 1970*

ABSTRACT: The structure of isotactic poly(methyl methacrylate) in the crystalline state was analyzed by the use of X-ray diffraction and far-infrared spectroscopic methods. At the first stage, the results of the conformational analysis, cylindrical Patterson function, and molecular structure factor calculation have led two types of helix models, of which the main difference lies in the conformation of the side chain. For both models the main chain is composed of a (5/1) helix containing five chemical units and one turn in the fiber identity period (the internal rotation angles; $\tau_1 = 180°$ and $\tau_2 = -108°$). Finally, one of these models has been found to be more reasonable from the far-infrared spectroscopy and normal coordinate treatment. The internal rotation angles of the side chain for this model are $\tau_3 = -24°$ and $\tau_4 = 171°$ in CH_3–C_{τ_3}–CO_{τ_4}–O–CH_3 and the α-CH_3 group points outward from the helix.

Poly(methyl methacrylate) (PMMA) can be prepared as samples from highly isotactic to syndiotactic depending upon the polymerization condition. This polymer has been noted for its importance from the viewpoint of nmr spectroscopy and mechanism of polymerization. The configuration, *i.e.*, isotactic or syndiotactic, was determined by nmr by noticing the absorption of methylene protons.[1,2]

The molecular conformation or crystal structure, however, has not yet been settled. Stroupe and Hughes[3] proposed a (5/2) helix model for isotactic PMMA. Here (5/2) denotes a helix which contains five chemical units and turns twice in the fiber identity period. Liquori and his coworkers[4] studied the ultraviolet spectrum of a dioxane solution of isotactic PMMA at various temperatures, and from this result and also from conformational analysis they suggested that the chain transforms from (5/1) to (5/2) helix at 43°. Furthermore, Liquori, *et al.*,[5] reported the formation of a crystalline complex of syndiotactic PMMA and isotactic PMMA with the mole ratio of 2:1.

In their article they noted that the Fourier transform of (5/2) helix was found to be inconsistent with the intensity distribution of the fiber photograph of isotactic PMMA; however, they have not reported further detailed results.

We have studied the structure of isotactic PMMA by the use of X-ray diffraction and far-infrared spectroscopy. From the results of the conformational analysis, cylindrical Patterson function, and molecular structure factor calculation, the possible models have been restricted to two types of (5/1) helices, one of which was finally found to be more reasonable from the far-infrared spectroscopic method.

(1) F. A. Bovey and G. V. D. Tiers, *J. Polym. Sci.*, **44**, 173 (1960).

(2) A. Nishioka, H. Watanabe, K. Abe, and Y. Sono, *ibid.*, **48**, 241 (1960).

(3) J. D. Stroupe and R. E. Hughes, *J. Amer. Chem. Soc.*, **80**, 2341 (1958).

(4) M. D'alagni, P. De Santis, A. M. Liquori, and M. Savino, *J. Polym. Sci., Part B*, **2**, 925 (1964).

(5) A. M. Liquori, Q. Anzuino, V. M. Coiro, M. D'alagni, P. De Santis, and M. Savino, *Nature (London)*, **206**, 358 (1965).